RSC Advances

ROYAL SOCIETY OF CHEMISTRY

www.rsc.org/advances

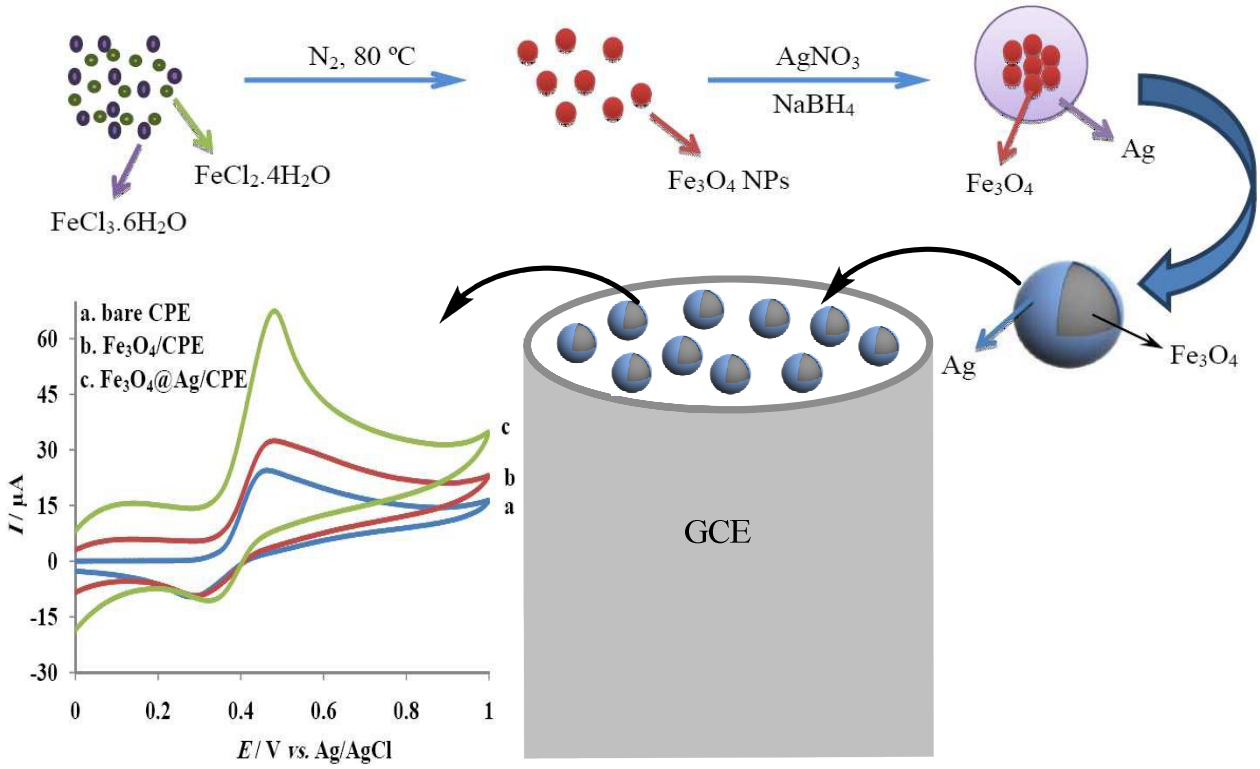

Fe_3O_4@Ag core/shell MNPs were used for modification of carbon paste electrode and the modified electrode was utilized for electrochemical determination of olanzapine.

Differential pulse stripping voltammetric determination of the antipsychotic medication olanzapine at a magnetic nano-composite with a core-shell structure

Majid Arvand*, Setareh Orangpour and Navid Ghodsi

Electroanalytical Chemistry Laboratory, Faculty of Science, University of Guilan, Namjoo Street, P.O. Box: 1914, Rasht, Iran

*Corresponding author. Tel.: +98131 3233262, fax: +98 131 3233262

E-mail address: arvand@guilan.ac.ir (M. Arvand)

Abstract

In this work, an electrochemical sensor based on Fe_3O_4@Ag core/shell magnetic nanoparticles (MNPs) was used to investigate the electrochemical behaviour of olanzapine. The synthesised Fe_3O_4@Ag core/shell MNPs were characterised by X-ray powder diffraction (XRD), transmission electron microscope (TEM) and scanning electron microscope (SEM). Fe_3O_4@Ag core/shell MNPs were used for modification of carbon paste electrode (CPE) and the nano-composite modified electrode (Fe_3O_4@Ag|CPE) was utilised for electrochemical investigation of olanzapine. Fe_3O_4@Ag|CPE led to an enhancement in electron transfer rate (ΔE_p = 141 mV) and showed good electrocatalytic activity for oxidation of olanzapine. Fe_3O_4@Ag core/shell MNPs also led to a 5.4-fold enlarged effective electrode surface area. The proposed electrode showed good linearity between the anodic peak current and the concentration of olanzapine at two concentration ranges of 0.39–1.38 and 1.38–38.4 μmol L^{-1} and the detection limit was calculated to be 0.0018 μmol L^{-1}. The modified electrode was used for determination of olanzapine in blood serum and plasma of schizophrenia patient.

Keywords: Fe_3O_4@Ag core/shell magnetic nanoparticles; Coprecipitation; Olanzapine; Differential pulse voltammetry

1. Introduction

Olanzapine (2-methyl-4-[4-methyl-1-piperazinyl]-10H-thieno[2,3-b][1,5] benzodiazepine) (OLZ, Figure 1) is a useful neuroleptic drug for refractory schizophrenia and acute mania patients.[1] Approximately 1.5% of the global population are suffering from schizophrenia disorder and OLZ is a common medication prescribed for this disease.[2,3] OLZ has an effect on the long-term behaviour of schizophrenia patients, for example, improvement of verbal learning and memory, verbal fluency and executive functions.[4] The reassessment of the performance of OLZ showed much less extra-pyramidal effect than other psychiatric medicines during the stable phase of the disease.[5] Dose and administration time are two important parameters of OLZ that have an influence on schizophrenia patients. Although there are much reduced symptoms after administering OLZ, compared to other drugs, some patients have shown side effects including change in vision, loss of balance, drooling, mask-like face and restlessness.[6] This antipsychotic medicine is a drug that has sustained-mood properties and reduces aggressive treatment, agitation, hostility in schizophrenia patients.[7] Therefore, OLZ is useful for managing acute aggression or agitation.[8]

There are different methods for the determination of OLZ in biological samples such as non-aqueous titrimetry and UV-spectrophotometry,[9] visible spectrophotometry,[10] flow injection spectrophotometry,[11] high performance liquid chromatography[12] and electrochemistry.[13] Due to the low cost, high sensitivity and less time requirement, electrochemical methods are preferred. Owing to its low electroactivity,[14] the electrochemical sensing of OLZ requires the sensing surface to be modified by a material that would enhance the electron transfer rate, decrease electrode fouling and increase the linear relation between current intensity and concentration of analyte.[15]

Please insert Figure 1 here

There are different kinds of nanomaterials which can be used for modifying of the surface of electrochemical sensors. In recent years, magnetic nanoparticles (MNPs) have been widely applied to different fields such as mineral separation,[16] magnetic storage devices,[17] catalysis, magnetic refrigeration system,[18] heat transfer application in drug delivery system,[19] magnetic resonance imaging,[20] cancer therapy,[21] magnetic cell separation,[22] and electrochemical sensors.[23] Among MNPs, magnetite (Fe_3O_4) has been widely used for fabrication of electrochemical sensors because of its excellent biocompatibility, super paramagnetic property, low toxicity and easy preparation compared to other nanomaterials such as gold nanoparticles or carbon nanotubes.[24–26] It has also been reported that these kind of particles could favorably interact with biological compounds by some active groups such as -OH, -COOH and -NH_2.[27]

There are several methods used for the synthesis of Fe_3O_4 MNPs such as thermal decomposition of alkaline solution of Fe(III) chelate in the presence of hydrazine,[28] sonochemical decomposition of hydrolyzed Fe(II) salt[29] and coprecipitation of ferrous (Fe(II)) and ferric (Fe(III)) ions. Among these methods, coprecipitation technique has some advantages including ease of performance, less time and solvent consumption.[30] However, Fe_3O_4 nanoparticles may not be very useful in biomedical and technological applications because they tend to aggregate to minimize surface energy. They have large surface-to-volume ratios and strong dipole-dipole attraction between particles, which lead to weakening of their magnetic property, and they have limited functional groups for selective binding.[31] To prevent these self-aggregations and to improve their chemical stability, the surface of Fe_3O_4 MNPs can be modified and protected using materials such as polymers,[32,33] metals[34] and metal oxides.[35] In some reports,

silver,[36] Au,[37] ZnO,[38] Al_2O_3[39] and polypyrrole[40] were used as a protective layer on Fe_3O_4 MNPs. Among these materials, silver nanoparticles (Ag NPs) have received much attention because of their unique properties, for example, high conductivity, high stability in various pH, nontoxicity, biocompatibility and electro-catalytic effect. Ag NPs lead to an enlargement in the surface to volume ratio and they minimise aggregation of Fe_3O_4 MNPs.[36] Therefore, these Ag NPs protected Fe_3O_4 MNPs (denoted as Fe_3O_4@Ag core/shell MNPs) can be utilised as a promising material for the modification of electrochemical biosensors. To our knowledge, no study has reported the electrocatalytic oxidation of OLZ using Fe_3O_4@Ag core/shell MNPs modified carbon paste electrode (Fe_3O_4@Ag|CPE).

In the present work, a coprecipitation method was utilised to synthesis of Fe_3O_4 MNPs and the prepared MNPs were coated by Ag NPs. The synthesized Fe_3O_4@Ag core/shell MNPs were utilised to modify the surface of carbon paste electrode. The mechanism of the electrode process was investigated and the effect of accumulation time and potential was studied. After optimisation of the electrochemical parameters, OLZ present in the serum and plasma of a schizophrenia patient was quantitatively determined and the results were compared with a reference method, which indicates that the proposed procedure is simple, cheap, rapid, selective and sensitive.

2. Experimental

2.1 Apparatus and reagents

Electrochemical experiments were carried out using a PalmSens analyser equipped with PSTrace 2.4 software. A three-electrode system consisting of a modified carbon paste electrode as a working electrode, a saturated Ag|AgCl reference electrode and a platinum wire counter

electrode was used in all electrochemical studies. A model CM10 transmission electron microscope (TEM, Philips) and a LEO 1430VP model scanning electron microscope (SEM) were used to characterise the size and morphology of the synthesised MNPs, respectively. A Philips PW1840 diffractometer with CuK_α radiation was used to record the X-ray patterns of synthesised MNPs. The UV-Vis spectrophotometer used for validating the method was obtained from Shimadzu (Japan).

All chemical materials were of analytical grade and used without further purification. Ferric chloride ($FeCl_3.6H_2O$) and ferrous chloride ($FeCl_2.4H_2O$) were obtained from Sigma Company. Ammonia (99.99%), silver nitrate ($AgNO_3$) and sodium borohydride ($NaBH_4$) were purchased from Merck (Darmstadt, Germany). OLZ was obtained from Sobhan Pharmaceutical Company (Rasht, Iran). An acetate buffer (0.1 mol L^{-1}) was prepared by mixing sodium acetate (0.1 mol L^{-1}) and acetic acid (0.1 mol L^{-1}), and adjusting the solution pH using a Metrohm 827 pH electrode and meter. All solutions were prepared using deionised water.

2.2 Preparation of Fe_3O_4 MNPs

Fe_3O_4 MNPs were synthesised by chemical coprecipitation of Fe(III) and Fe(II) ions.[41] In a typical procedure, 2.0 g of $FeCl_3.6H_2O$ and 2.25 g of $FeCl_2.4H_2O$ were dissolved in 100 mL doubly distilled water in a three-necked flask under N_2 atmosphere and stirred vigorously at 80 °C for 30 min. Chemical precipitation was achieved at 25 °C under vigorous stirring by adding NH_4OH solution (25% v/v). During the reaction process, the pH was maintained at about 10. The precipitates were heated at 80 °C for 30 min and then washed several times with water and ethanol until the solution was nearly neutral, and then dried in a vacuum oven at 70 °C before being stored in glass vials.

2.3 Synthesis of Fe_3O_4@Ag core/shell MNPs

In our work, 0.2 g of synthesised Fe_3O_4 MNPs and 4 mL of $AgNO_3$ (0.064 mmol L^{-1}) were added into 14 mL of deionised water and stirred for 24 h. The supernatant was removed by magnetic separation. Next, 5 mL of 0.32 mmol L^{-1} of freshly prepared $NaBH_4$ solution was added until the color of suspension changed from black to greyish green. The obtained Fe_3O_4@Ag core/shell MNPs were separated by centrifuging, and dried under high vacuum (Scheme 1).[42]

Please insert Scheme 1 here

2.4 The preparation of working electrode

An appropriate mass of the synthesised Fe_3O_4@Ag core/shell MNPs was mixed with a desired quantity of graphite powder and paraffin oil. Then this mixture was thoroughly blended to achieve a homogenous nano-composite paste. The prepared modified carbon paste was packed into an Ertalon tube and a copper wire was utilised for electrical connection.

2.5 Experimental procedure

In stripping voltammetric analysis, all analyte solutions were prepared in pH 4.3 acetate buffer. A magnetic stirrer at a rate of 400 rpm was used to promote the convective transport of the analyte to the carbon paste electrode during the accumulation period. An accumulation potential of +0.25 V was applied to the Fe_3O_4@Ag|CPE for 150 s. At the end of the accumulation period, the stirring was stopped, and a 15 s rest period was allowed for the solution to become quiescent. A differential pulse stripping voltammogram (5 mV step potential, 50 ms pulse width, 500 ms

pulse period and 50 mV pulse amplitude) was then recorded by applying a positive scan from +0.28 to +0.48 V.

2.6 Sample preparation

2.6.1 Preparation of plasma and serum samples

A serum sample was obtained from a patient with schizophrenia condition. In these experiments, a series of 100 mL OLZ solutions of different concentration spiked with 10 μL of each human serum sample was prepared using pH 4.3 acetate buffer. These OLZ solutions were then quantitatively analysed.

2.6.2 Preparation of pharmaceutical samples

Experimentally, 15 tablets of OLZ, each containing either 5 or 15 mg of OLZ, were randomly selected and weighed. The tablets were well powdered and mixed using a pestle and mortar. Next, 2.1 g of homogenous powder of each dose tablet was dissolved in HCl (0.1 mol L^{-1}). After removing any insoluble residues, the solution was transferred to a 25 mL volumetric flask and diluted to volume using pH 4.3 acetate buffer.

3. Results and discussion

3.1 Characterisation of Fe_3O_4@Ag core/shell MNPs

To confirm the formation of Fe_3O_4 and Fe_3O_4@Ag core/shell MNPs, typical transmission electron micrographs of synthesised colloidal solutions are shown in Figure 2(A) and (B). In Figure 2(A), spherical Fe_3O_4 MNPs with a mean diameter of around 10 nm were obtained. After modifying Fe_3O_4 MNPs with Ag NPs, a core/shell structure with a mean diameter around 25 nm

is observable in Figure 2(B), which illustrates the presence of Ag NPs around of the Fe_3O_4 MNPs. To study the surface morphology and the effect of modification of CPE with Fe_3O_4@Ag MNPs, scanning electron micrographs before and after the addition of Fe_3O_4@Ag MNPs are shown in Figure 2(C) and (D), respectively. A comparison between Figure 2(C) and Figure 2(D) reveals that the surface of graphite paste was relatively smooth, but this surface appeared rugged and crumpled after Fe_3O_4@Ag MNPs was immobilised, adding active sites to the electrode surface. The crystalline structure of the Fe_3O_4@Ag nanoparticles synthesised was characterised by X-ray diffraction and the results obtained are shown in Figure 2(E). By comparing to the reference X-ray diffraction pattern of Fe_3O_4 (JCPDS No. 75-0033) and Ag crystal (JCPDS No. 03-0921), the reflection peaks at 30.53, 35.37, 39.05, 43.37, 57.27 and 62.55 were correspondingly assigned to those of Fe_3O_4 (220), (311), (511), and Ag (111), (200) and (220). The reflection peak position confirmed that Fe_3O_4@Ag MNPs were obtained.

Please insert Figure 2 here

3.2 Electrochemical behaviour of modified electrodes

In studying the electrochemical behaviour of a Fe_3O_4@Ag|CPE, cyclic voltammetry of 5 mmol L^{-1} $[Fe(CN)_6]^{3-/4-}$ was conducted at a CPE (a), Fe_3O_4|CPE (b) and Fe_3O_4@Ag|CPE (c) in 0.1 mol L^{-1} KCl and the voltammograms obtained are shown in Figure 3. Compared to the voltammogram at the CPE, the voltammogram obtained at the Fe_3O_4|CPE displayed a 37.5% larger anodic peak current and a 61.7% larger cathodic peak current. Also, a peak separation of 337 mV was obtained in the voltammogram at the CPE, compared to the corresponding peak separation of 225 mV obtained at the Fe_3O_4|CPE. All these results support an electrocatalytic effect of Fe_3O_4 MNPs for the redox reaction of $[Fe(CN)_6]^{3-/4-}$. According to the cyclic

voltammogram of Fe_3O_4@Ag|CPE, the anodic and cathodic peak currents for $[Fe(CN)_6]^{3-/4-}$ at the Fe_3O_4@Ag|CPE are 21% and 27.8% higher than those at the Fe_3O_4|CPE, respectively, and the anodic and cathodic peak separation for this electrode is at its lowest value (190 mV). All these results support an enhanced electrocatalytic effect of MNPs at the modified electrodes arising from the increased surface-to-volume ratio and conductivity.

The surface area of the modified electrode was estimated based on the cyclic voltammetry of 5 mmol L^{-1} $[Fe(CN)_6]^{3-/4-}$ in 0.1 mol L^{-1} KCl at different scan rates.[43] For a reversible process, the following Randles-Sevcik formula can be used.[44]

$$I_{pa} = 0.4463(F^3/RT)^{1/2} n^{3/2} AD^{1/2} C\nu^{1/2} \quad (1)$$

where I_{pa} denotes the anodic peak current, A is surface area of the electrode (cm^2), n is number of exchanged electron, C is concentration of $[Fe(CN)_6]^{3-/4-}$, ν is scan rate (V s^{-1}) and D is diffusion coefficient of the $[Fe(CN)_6]^{3-/4-}$ ($D = 7.6 \times 10^{-6}$ cm^2 s^{-1}).[45] From the Equation (1) the surface area of the modified electrode was estimated to be 0.076 cm^2. The same experiment was done for CPE and its surface area was evaluated to be 0.0141 cm^2. These results indicate that the presence of Fe_3O_4@Ag MNPs led to a 5.4-fold enlarged effective electrode surface area.

Please insert Figure 3 here

3.3 Electrochemical behaviour of OLZ

Electrochemical behaviour of OLZ was studied at the surface of CPE, Fe_3O_4|CPE and Fe_3O_4@Ag|CPE and the cyclic voltammograms obtained are shown in Figure 4. In all three voltammograms, an oxidation peak between 0.46 V and 0.48 V and a reduction peak between 0.28 V and 0.34 V were observed. They are attributable to the redox reaction of tertiary amine functional group of OLZ. With consideration to Figure 4, it can be interpreted that after addition

of Fe_3O_4 MNPs, the separation between anodic and cathodic peaks (ΔE_p) decreased and the peak currents increased. This means that Fe_3O_4 MNPs show electrocatalytic effect on the electro-oxidation of OLZ. When the surface of the CPE was modified by Fe_3O_4@Ag core/shell MNPs, the ΔE_p for the OLZ reaction was estimated to be 141 mV, compared to 170 mV at a Fe_3O_4|CPE and 180 mV at a CPE. Meanwhile, the corresponding peak current increased by 15% at the Fe_3O_4@Ag|CPE compared to the Fe_3O_4|CPE and 57% compared to the CPE. Therefore, it can be concluded that Fe_3O_4@Ag core/shell MNPs led to facilitation in electron transfer process of OLZ and enhanced the conductivity of the electrode.

Please insert Figure 4 here

3.4 Effect of pH

The concentration of proton plays a main role in the electro-oxidation of OLZ, because it affects the peak currents and potentials. Figure 5 shows the cyclic voltammograms of 2 μmol L^{-1} OLZ in pH 4.3 acetate buffer of different pH values. As shown in the inset of Figure 5, when the pH was increased from 4 to 5.6, the oxidation peak current initially rose and then decreased. Meanwhile, the anodic peak potential decreased linearly with pH and this is represented by the expression, E_{pa} (V) = –0.062(±0.002)pH + 0.689(±0.011) with R^2 = 0.999 (n=5). Therefore, a slope of 0.062 V is in good agreement with the expected 0.059 V for two electron-two proton transfer. Therefore, the number of transferred protons and electrons in electrochemical oxidation of OLZ are equal. As can be seen from the inset of Figure 5, at higher pH values, OLZ can be oxidised at a lower voltage, but the maximum anodic peak current was obtained at pH value of 4.3. Hence, this pH was chosen as optimum value for the rest of study.

Please insert Figure 5 here

3.5 Effect of the quantity of Fe_3O_4@Ag MNPs

The quantity of Fe_3O_4@Ag MNPs as a modifier has an effect on the electrochemical responses. Figure S1 shows cyclic voltammograms of OLZ at a Fe_3O_4@Ag|CPE surface with a Fe_3O_4@Ag to graphite ratio of 0.083%, 0.12%, 0.21% and 0.24% (w/w), respectively. By increasing the quantity of Fe_3O_4@Ag MNPs, the anodic peak current increased firstly and then it decreased. So the ratio of 0.12 (w/w%) was selected as the optimum amount for the rest of the experiments.

3.6 Effect of scan rate

Cyclic voltammograms of 0.1 mmol L^{-1} OLZ at the surface of Fe_3O_4@Ag|CPE at different scan rates (0.01 to 0.14 V s^{-1}) are shown in Figure 6. It is seen that by increasing the scan rate the anodic and cathodic peak currents increase linearly (inset of Figure 6) and they can be represented by I_{pa} (μA) = 61.97(±1.48)υ (V s^{-1}) + 2.927(±0.122) (R^2 = 0.995, n = 10) and I_{pc} (μA) = –18.78(±0.62)υ (V s^{-1}) – 0.3492(±0.0513) (R^2 = 0.991, n = 10) for anodic and cathodic peak currents, respectively. It can be concluded that the electrochemical reaction of OLZ at the surface of Fe_3O_4@Ag|CPE is controlled by an adsorption process. In the potential scan rate range from 10–140 mV s^{-1}, the numbers of electrons transferred in electrode reaction (n) was calculated directly by using Eq. (2),[45] in which Q is the charge (C mol^{-1}) consumed by the surface process as calculated by the integration of the surface area under the peak.

$$n = \frac{4I_pRT}{FQv} \quad (2)$$

Based on the slope of a peak current versus scan rate plot, the number of electrons transferred was estimated to be 2. Therefore two protons–two electrons transfer can be assumed for electro-oxidation process of OLZ.

Please insert Figure 6 here

3.7 Influence of accumulation time and potential

Because the electro-oxidation process of OLZ on the surface of Fe_3O_4@Ag|CPE is controlled by an adsorption process, the effects of accumulation time (t_{acc}) and accumulation potential (E_{acc}) on the response of electrode should be evaluated. Figure S2(A) illustrates that by increasing the accumulation potential from 0 to 0.35 V, the anodic peak current increased and reached to its highest value at the potential of 0.25 V, then decreased, so the E_{acc} of 0.25 V was selected as optimum value. Figure S2(B) shows the dependence of I_{pa} to t_{acc}. It can be observed that by increasing t_{acc} at E_{acc} of 0.25 V, the anodic peak current reached its maximum amount at t_{acc} of 150 s, which indicated that, for a period longer than 150 s, the surface of the Fe_3O_4@Ag|CPE was saturated with OLZ and the number of active sites on electrode was reduced. Thus, the E_{acc} of 0.25 V and t_{acc} of 150 s were utilised for the rest of studies.

3.8 Calibration study

The proposed method was employed for electrochemical determination of OLZ. In this respect, the relationship between the anodic peak currents and the concentrations of OLZ was studied using differential pulse voltammetry (DPV) under the optimum conditions and the results obtained are shown in Figure 7. The inset of Figure 7 shows two linear ranges between anodic peak currents and the concentrations of OLZ of 0.39–1.38 and 1.38–38.4 μmol L^{-1}. The detection limit (DL), which is defined as the concentration of the sample yielding a signal equal to the blank signal three times its standard deviation (S/N=3), was estimated to be 0.0018 μmol L^{-1}. Based on the slope of each calibration equation $I_{pa}(\mu A) = 0.502(\pm 0.004)C$ (μmol L^{-1}) +

0.0854(±0.0013) and I_{pa}(μA) = 0.0924(±0.0023)C (μmol L^{-1}) + 0.375(±0.026), the sensitivity of this electrode was obtained to be 0.502 and 0.0924 μA L μmol^{-1}, respectively. A comparison between the analytical performance of the present modified electrode and several previously reported electrodes for the determination of OLZ are given in Table 1. As can be seen from Table 1 the DL of the proposed electrode is lower than the others. The proposed method has wide linear dynamic range (LDR) and shows good sensitivity.

Please insert Figure 7 here

Please insert Table 1 here

3.9 Stability, repeatability and reproducibility

The stability and reproducibility of the Fe_3O_4@Ag|CPE were also studied. The DPV experiments were carried out using the modified electrode under the same operation conditions (pH 4.3, t_{acc} = 150 s, E_{acc} = 0.25 V, modifier to graphite ratio of 0.12% (w/w)). The anodic peak current of OLZ was observed to have decreased by ~2% after storing the electrode at room temperature for one week. Only a minimal decrease of current with a relative standard deviation (RSD) of 0.8% was observed after a month and the RSD of 1.23% for three consecutive measurements of 5 μmol L^{-1} OLZ was obtained. Five Fe_3O_4@Ag|CPEs were fabricated with the same procedure and were applied to the determination of 5 μmol L^{-1} OLZ with a relative standard deviation of 2.76%. These results suggest excellent repeatability and reproducibility for the Fe_3O_4@Ag|CPE.

3.10 Interference effect

The influence of various foreign compounds and ions on the determination of 100 μmol L^{-1} of OLZ in acetate buffer (pH 4.3) was investigated by an amperometric method. The results,

displayed in Figure 8, show that the presence of lactose, cysteine, clozapine (CLZ), folic acid (FA), ascorbic acid (AA), Na^+, K^+, Mg^{2+}, Ca^{2+} have not significantly influenced the height of the currents (signal change of less than 7%). The same concentration of uric acid (UA) showed distinct peak in the presence of OLZ. Figure S3 demonstrates the DPV of the mixture of 7.4 μmol L^{-1} OLZ and 7.4 μmol L^{-1} UA in acetate buffer (pH 4.3) on a modified carbon paste electrode. There are two anodic peaks at around 0.28 and 0.39 V, which were attributed to the oxidation of UA and OLZ with a 0.11 V separation between the two peaks, indicating two resolved peaks for the simultaneous electrochemical determination of UA and OLZ. Further work is being conducted in our laboratory.

Please insert Figure 8 here

3.11 Real-life sample analysis

In order to study the validity of the proposed method, the Fe_3O_4@Ag|CPE was utilised to quantify the concentration of OLZ in tablets and blood serum and plasma of schizophrenia patient treated by OLZ. Then, the standard addition method was applied to the quantitative determination of OLZ in serum and plasma via DPV. UV-Vis spectrophotometry method was used as the reference method. The measurements were done at λ = 251 nm. Figure S4 shows the typical DPVs of the serum sample with various concentrations of OLZ. The results are shown in Tables 2 and 3. The results indicate that there is a good relation between analyte content and the determined amount, which confirms that the proposed method is suitable for the determination of OLZ in real-life samples. *F*-test was then used to examine if the standard deviations of the results obtained using the Fe_3O_4@Ag|CPE and the reference technique of UV-Vis spectrophotometry were significantly different. Similarly, *t*-test was conducted to examine if the mean OLZ

concentrations obtained by the two techniques were significantly different. At the 95% of the confidence level, the test statistic values of both the *F*-test and *t*-test were lower than the corresponding critical values (n = 3), indicating no significant difference between the proposed DPV method and reference UV-Vis method.

Please insert Table 2 here

Please insert Table 3 here

4 Conclusions

In this article, Fe_3O_4@Ag core/shell MNPs were synthesised using a coprecipitation method and utilised for modification of carbon paste electrodes for electrochemical determination of OLZ. The experimental results indicated that the core/shell magnetic nanostructures improved the conductivity and the surface area of CPE. The proposed electrode decreased the peak to peak potential for oxidation of OLZ and increased the peak currents. At optimised conditions, anodic peak currents had suitable linear relation with concentration of OLZ at range of 0.39–38.4 μmol L^{-1} and DL was about 0.0018 μmol L^{-1}. This method provided a simple, rapid and sensitive technique for measurement of OLZ in biological samples.

Acknowledgement

The authors are thankful to the post-graduate office of Guilan University for the support of this work.

Compliance with ethical standards

Ethical approval: All procedures performed in studies involving human participants were in accordance with the ethical standards of the institutional and/or national research committee and with the 1964 Helsinki declaration and its later amendments or comparable ethical standards.

This article does not contain any studies with animals performed by any of the authors.

Informed consent: Informed consent was obtained from all individual participants included in the study.

References

1 P. L. McCormack and L. R. Wiseman, *Drug*, 2004, **64**, 2709–2726.

2 R. Freedman, *New Engl. J. Med*., 2003, **349**, 1738–1749.

3 S. Weinbrenner, H. J. Assion, T. Stargardt, R. Busse, G. Juckel and C. A. Gericke, *Pharmacopsychiatry*, 2009, **42**, 66–71.

4 T. Sharma, C. Hughes, W. Soni and V. Kumari, *Psychopharmacology*, 2003, **169**, 398–403.

5 F. Rouillon, F. Chartier and I. Gasquet, *Eur. Neuropsychopharmacol*., 2008, **18**, 646–652.

6 H. N. Boyda, L. Tse, R. M. Procyshyn, D. Wong, T. K. Wu, C. C. Pang and A. M. Barr, *Prog. Neuropsychopharmacol. Biol. Psychiatry*, 2010, **34**, 945–954.

7 I. Bitter, P. Czobor, M. Dossenbach and J. Volavka, *J. Eur. Psychiatry*, 2005, **20**, 403–408.

8 B. J. Kinon, S. M. Roychowdhury, D. R. Milton and A. L. Hill, *J. Clin. Psychiatry*, 2001, **62**, 17–21.

9 S. Firdous, T. Aman and A. Nisa, *J. Chem. Soc. Pakistan*, 2005, **27**, 163–167.

10 K. V. Sivaprasad, J. M. R. kumar, M. V. V. N. Reddy, G. Prabhakar and D. G. Sankar, *Asian J. Chem*., 2003, **15**, 1127–1130.

11 A. Jasinska and E. Nalewajko, *Anal. Chim. Acta*, 2004, **508**, 165–170.

12 X. Xia and Z. Tao, *Zhongguo Yiyao Gongye Zazhi*, 2004, **35**, 46–48.

13 M. Arvand and B. Palizkar, *Mater. Sci. Eng. C*, 2013, **33**, 4876–4883.

14 G.M. Greenway and S. J. L. Dolman, *Analyst*, 1999, **124**, 759–762.

15 N. F. Atta, A. Galal and S. M. Azab, *Analyst*, 2011, **136**, 4682–4691.

16 Z. L. Liu, H. B. Wang, H. Q. Lu, G. H. Du, L. Peng, Y. Q. Du, S. M. Zhang and K. L. Yao, *J. Magn. Magn. Mater.*, 2004, **283**, 258–262.

17 J. Hu, G. Chen and M. C. Lo, *J. Environ. Eng.*, 2006, **132**, 702–715.

18 Y. C. Sharma and V. Srivastava, *J. Chem. Eng. Data*, 2010, **55**, 1441–1442.

19 Y. C. Sharma, V. Srivastava, C. H. Weng and S. N. Upadhyay, *Can. J. Chem. Eng*., 2009, **87**, 921–929.

20 Y. C. Chang and D. H. Chen, *Macromol. Biosci*., 2005, **5**, 254–261.

21 A. S. Teja and P. Y. Koh, *Progr. Cryst. Growth Character. Mater*., 2005, **55**, 22–45.

22 J. Zhou, W. Wu, D. Caruntu, M. H. Yu, A. Martin, J. F. Chen, C. J. O. Connor and W. L. Zhou, *J. Phys. Chem. C*, 2007, **111**, 17473–17477.

23 M. Arvand and M. Hassannezhad, *Mater. Sci. Eng. C*, 2014, **36**, 160–167.

24 Y. He, Q. Shen, J. Zheng, M. Wang and B. Liu, *Electrochim. Acta*, 2011, **56**, 2471–2476.

25 D. Lu, Y. Zhang, L. Wang, S. X. Lin, C. M. Wang and X. F. Chen, *Talanta*, 2012, **88**, 181–186.

26 U. Schwertmann and R. M. Cornell, *Iron Oxides in the Laboratory: Preparation and Characterization*, New York, Wiley-VCH, 1991.

27 J. M. Gong and X. Q. Lin, *Microchemical J.*, 2003, **75**, 51–57.

28 R. Vijayakumar, Y. Koltypin, I. Felner and A. Gedanken, *Mater. Sci. Eng. A*, 2000, **286**, 101–105.

29 T. Fried, G. Shemer and G. Markovich, *Adv. Mater.*, 2001, **13**, 1158–1161.

30 K. Nakatsuka, B. Jeyadevan and S. Neveu, *J. Magn. Magn. Mater*., 2002, **252**, 360–362.

31 X. Chen, J. Zhu, Z. Chen, C. Xu, Y. Wang and C. Yao, *Sens. Actuators B*, 2011, **159**, 220–228.

32 C. L. Pan, B. Hu, W. Li, Y. Sun, H. Ye and X. X. Zeng, *J. Mol. Catal. B: Enzym*., 2009, **61**, 208–215.

33 J. Lin and M. X. Wan, *J. Polym. Sci. Part A: Polym. Chem*., 2000, **38**, 2734–2739.

34 K. M. Yeo, J. Shin and I. S. Lee, *Chem. Commun*., 2008, **46**, 64–66.

35 K. M. Kant, K. Sethupathi and M. S. R. Rao, *J. Appl. Phys*., 2008, **103**, 23–28.

36 Y. Shujun, W. Qin, D. Bin, W. Dan, L. He, Y. Liangguo, M. Hongmin and Z. Yong, *Biosens. Bioelectron*., 2013, **48**, 224–229.

37 L. Yan, H. Ting, C. Chao, B. Ning, Y. C. Mei and G. H. Ying, *Electrochim. Acta*, 2011, **56**, 3238–3247.

38 W. Jiaqi, L. Hui and C. Kezheng, *Mater. Chem. Phys*., 2009, **114**, 30–32.

39 H. P. Peng, R. P. Liang and J. D. Qiu, *Biosens. Bioelectron*., 2011, **26**, 3005–3011.

40 K. M. Mangold, J. Schuster and C. Weidlich, *Electrochim. Acta*, 2011, **56**, 3616–3619.

41 M. H. Liao and D. H. Chen, *J. Mater. Chem*., 2002, **12**, 3654–3659.

42 S. Guo, D. Li, L. Zhang, J. Li and E. Wang, *Biomaterials*, 2009, **30**, 1881–1889.

43 M. Arvand and N. Ghodsi, *Sens. Actuators, B*, 2014, 204, 393–401.

44 J. C. Abbar and S. T. Nandibewoor, *Ind. Eng. Chem. Res.*, 2012, **51**, 111–118.

45 A. J. Bard and L. Faulkner, *Electrochemical Methods*, Wiley, New York, 1980.

46 D. Merli, D. Dondi, M. Pesavento and A. Profumo, *J. Electroanal. Chem.*, 2012, **683**, 103–111.

47 M. A. El-Shal, *Adv. Pharm. Bull*., 2013, **32**, 339–344.

48 M. H. Mashhadizadeh and E. Afshar, *Electroanalysis*, 2012, **24**, 2193–2202.

49 H. M. Ahmed, M. A. Mohamed and W. M. Salem, *Anal. Methods*, 2015, **7**, 581–589.

Table 1 Comparison of different modified electrodes for the determination of OLZ

Electrode	pH	LDR ($\mu mol\ L^{-1}$)	DL ($\mu mol\ L^{-1}$)	Sensitivity ($\mu A\ L\mu mol^{-1}$)	Method	Sample	Ref.
NH_2-TiO_2-MWCNTs/GCE[a]	5	0.64–32	0.3	0.09	SWV	Human blood serum and commercial tablet	13
(SWCNTS-COOH)-CME[b]	8.5	0.64–320	0.32	0.087	DPV	Pharmaceutical formulations and urine samples	46
GCE	2	0.03–4	0.01	–	DPV	Pharmaceutical dosage forms and biological samples	47
ZnSNP-MCPE[c]	7	20.0–50.0	–	–	DPV	Human urine samples	48
GNGLCP[d]	7	0.5–125	0.0036	0.251	DPV	Commercial tablet and human urine samples	49
Fe_3O_4@Ag|CPE	4.3	0.39–1.38 1.38–38.4	0.0018	0.5015	DPV	Pharmaceutical formulations and schizophrenia blood serum and plasma	This work

[a]Amine functionalized TiO_2/multi-walled carbon nanotubes/glassy carbon electrode; [b]Oxidized single walled carbon nanotubes/chemically modified electrode; [c]ZnS nanoparticles modified carbon paste electrode; [d]Gold nanoparticles/glutamine modified carbon paste electrode.

Table 2 Determination results of olanzapine in tablets

Sample	Amount labeled	Olanzapine (mg)		RSD	Recovery
	(mg/tablet)	Added	Found[a]	(%)	(%)
Olanzapine tablet	5	–	4.56 ± 0.12	2.63	91.2
	5	5	10.41 ± 0.09	0.86	108.2
Olanzapine tablet	15	–	14.83 ± 0.13	0.88	98.9
	15	15	28.51 ± 0.09	0.32	90.1

[a] $x = x \pm s_x$ for $n = 3$ and s_x denotes standard deviation.

Table 3 Comparison of OLZ concentration in real samples determined by the proposed and reference techniques

Sample	Olanzapine (μmol L^{-1})[a]				*t*-test[b]	*F*-test[c]
	Proposed method	RSD (%)	Reference method	RSD (%)		
Plasma	4.87 ± 0.13	2.67	5.02 ± 0.09	1.79	1.64	2.09
Serum	3.61 ± 0.15	4.16	3.86 ± 0.08	2.07	2.55	3.52

[a] $x = x \pm s_x$ for $n = 3$ and s_x denotes standard deviation.

[b] Tabulated *t*-value for 2° of freedom at *P* value of 0.05 is 4.30.

[c] Tabulated *F*-value for 2,2° of freedom at *P* value of 0.05 is 19.00.

Figure captions

Figure 1 Chemical structure of OLZ.

Figure 2 TEM images of Fe_3O_4 MNPs (A), Fe_3O_4@Ag|CPE (B); SEM images of Fe_3O_4@Ag|CPE (C), bare CPE (D); XRD for Fe_3O_4@Ag|CPE (E).

Figure 3 Cyclic voltammograms of the (a) bare CPE, (b) Fe_3O_4|CPE and (c) Fe_3O_4@Ag|CPE in 5 mmol L^{-1} $K_3[Fe(CN)_6]$ containing 0.1 mol L^{-1} KCl.

Figure 4 Cyclic voltammograms of blank 0.1 mol L^{-1} acetate buffer (pH 4.3) at Fe_3O_4@Ag|CPE (a); 5 μmol L^{-1} OLZ in 0.1 mol L^{-1} acetate buffer solution (pH 4.3) at bare CPE (b), Fe_3O_4|CPE (c) and Fe_3O_4@Ag|CPE (d). Scan rate is 0.1 V s^{-1}.

Figure 5 Influence of solution pH on the voltammograms of Fe_3O_4@Ag|CPE; pH 4.0, 4.3, 4.8, 5.1, 5.6. Inset: the influence of solution pH on I_{pa} and E_{pa} of OLZ. Scan rate is 0.1 V s^{-1}.

Figure 6 Cyclic voltammograms of 0.1 mmol L^{-1} OLZ at the surface of Fe_3O_4@Ag|CPE in 0.1 mol L^{-1} acetate buffer (pH 4.3) at different scan rates (0.01, 0.02, 0.03, 0.04, 0.06, 0.07, 0.1, 0.11, 0.12, 0.14 V s^{-1} from inner to outer). Inset: plots of peak currents *vs.* scan rate.

Figure 7 DPVs obtained for the oxidation of OLZ at different concentrations: (a) 0.0, (b) 0.22, (c) 0.45, (d) 0.79, (e) 0.89, (f) 1.18, (g) 1.38, (h) 2.15, (i) 2.72, (j) 5.66, (k) 7.40, (l) 19.6, (m) 29 and (m) 38.4 μmol L^{-1}. Voltammetric conditions: E_{acc} = +0.25 V, t_{acc} = 150 s, in acetate buffer (pH 4.3), step potential = 5 mV and modulation amplitude = 50 mV. Inset: the relation between the anodic peak currents and the concentrations of OLZ.

Figure 8 The amperometric response of the Fe_3O_4@Ag|CPE for various compounds (100 μmol L^{-1}) in acetate buffer (pH 4.3).

Scheme captions

Scheme 1 Schematic representation of the preparation process of Fe_3O_4@Ag core/shell MNPs.

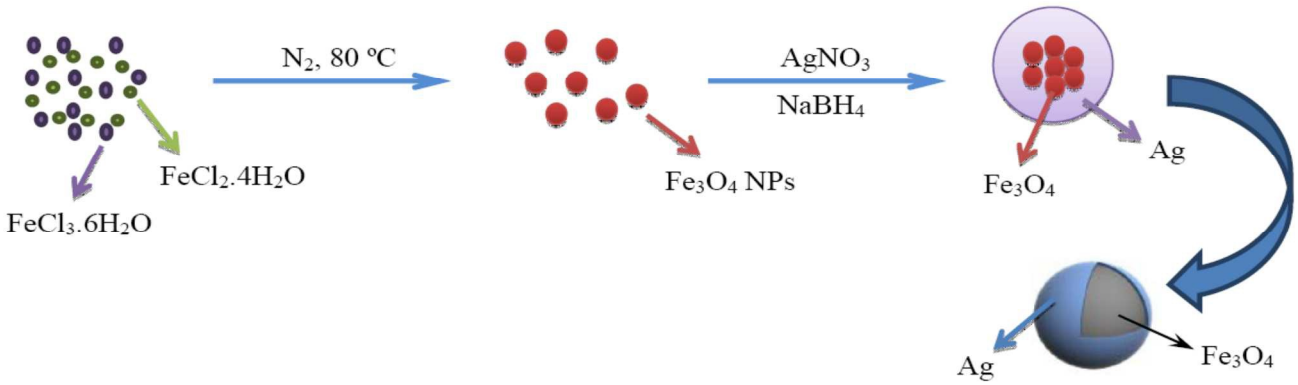

Scheme 1

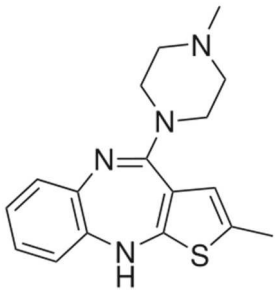

Figure 1

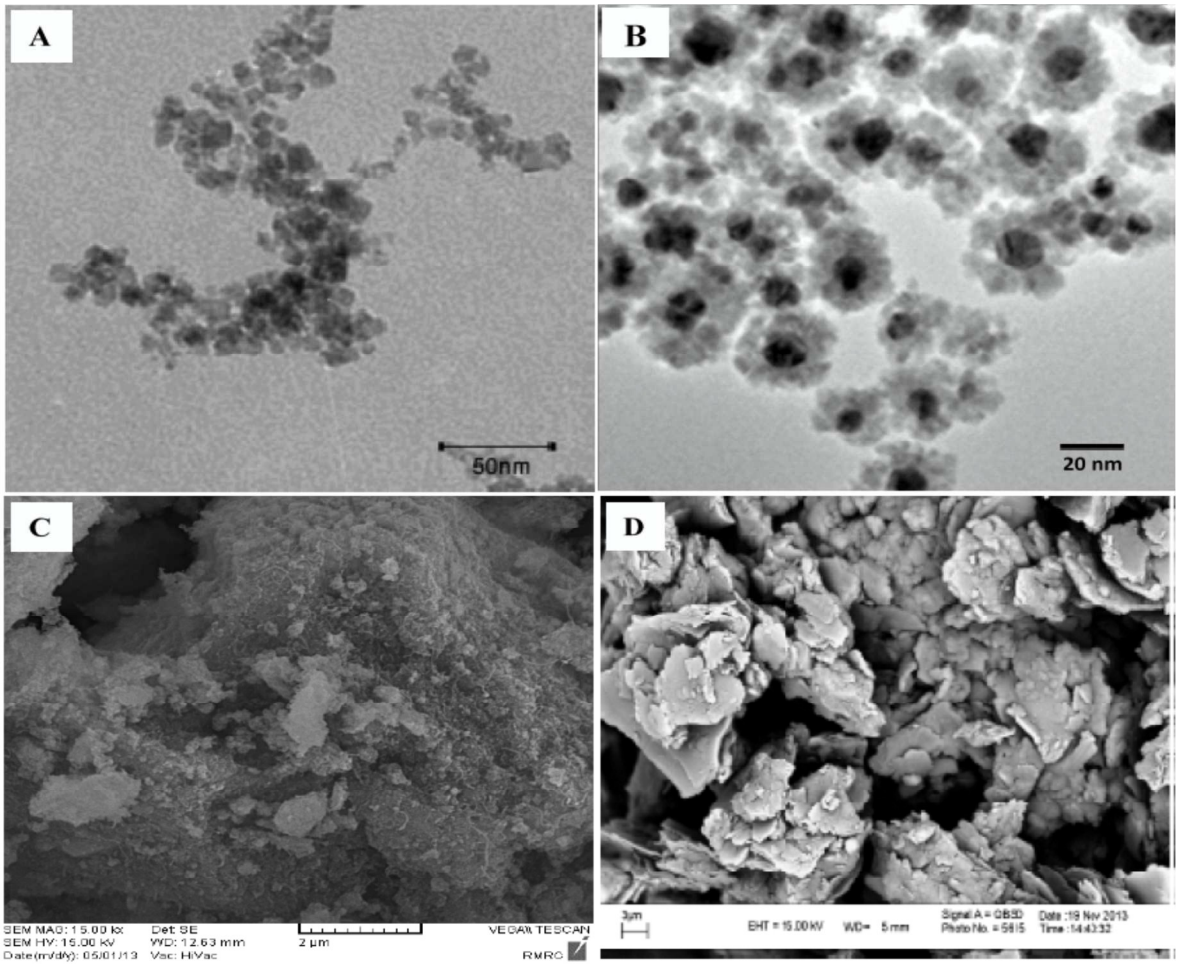

Figure 2

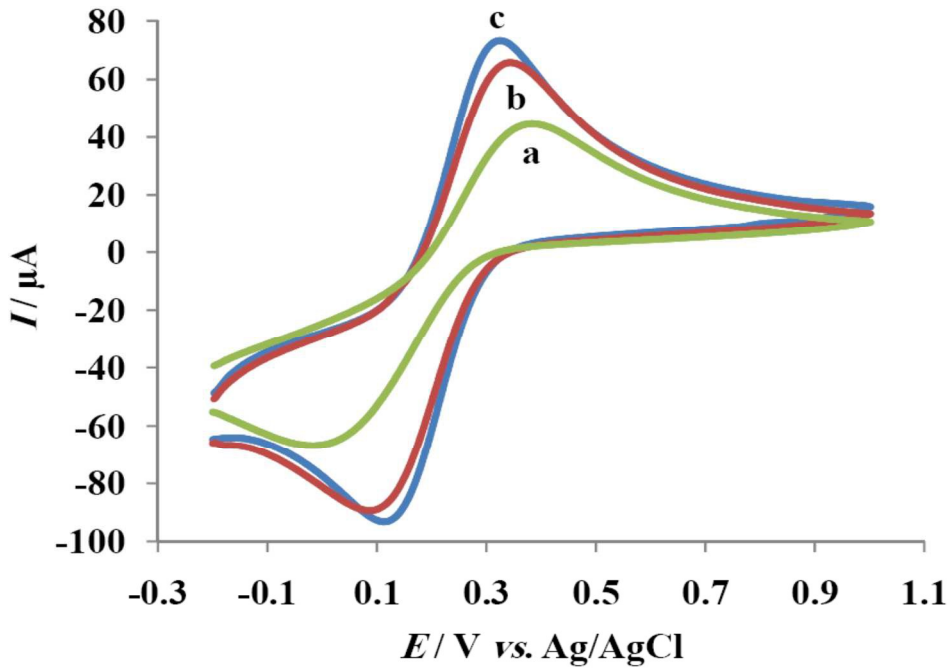

Figure 3

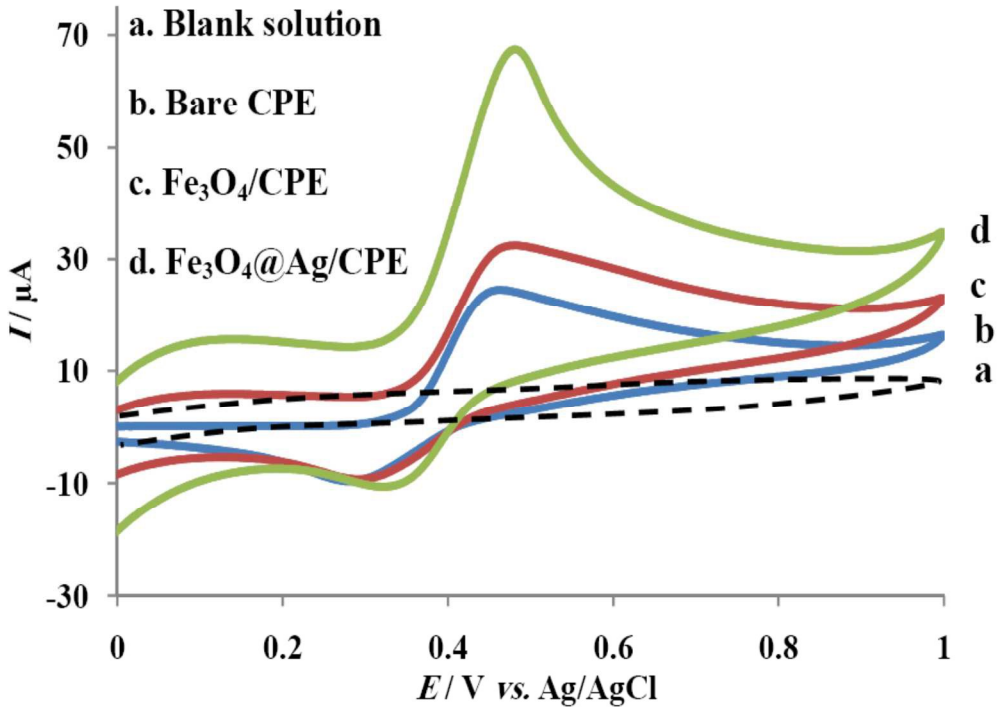

Figure 4

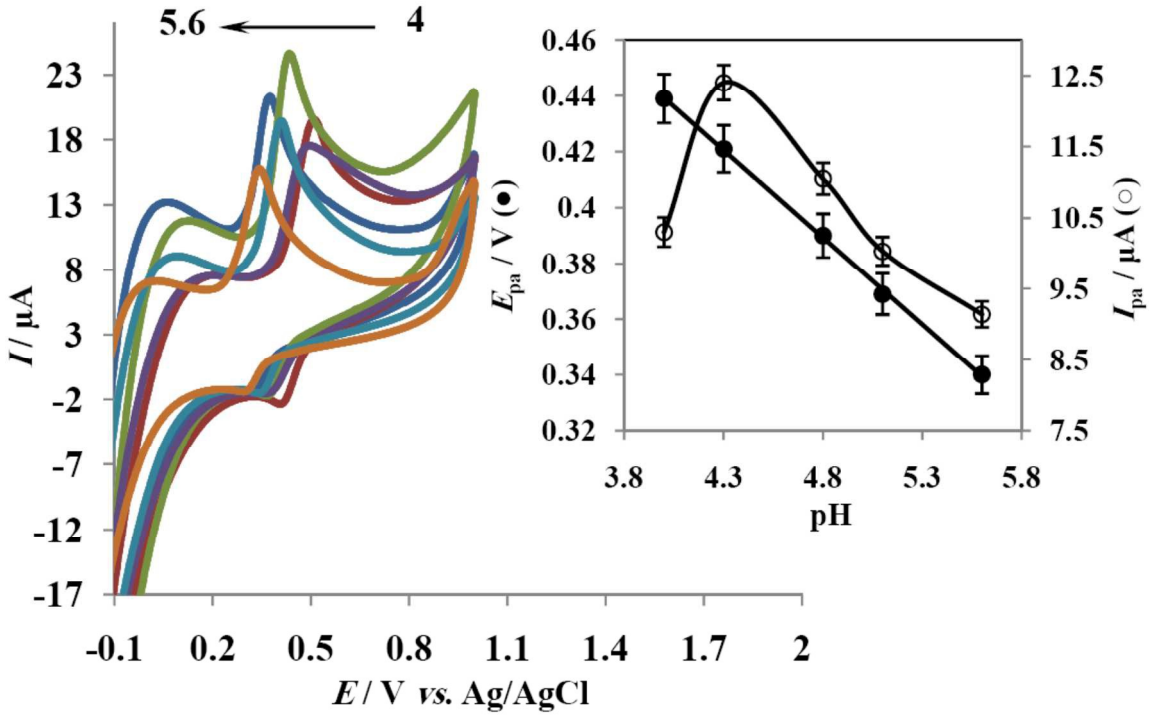

Figure 5

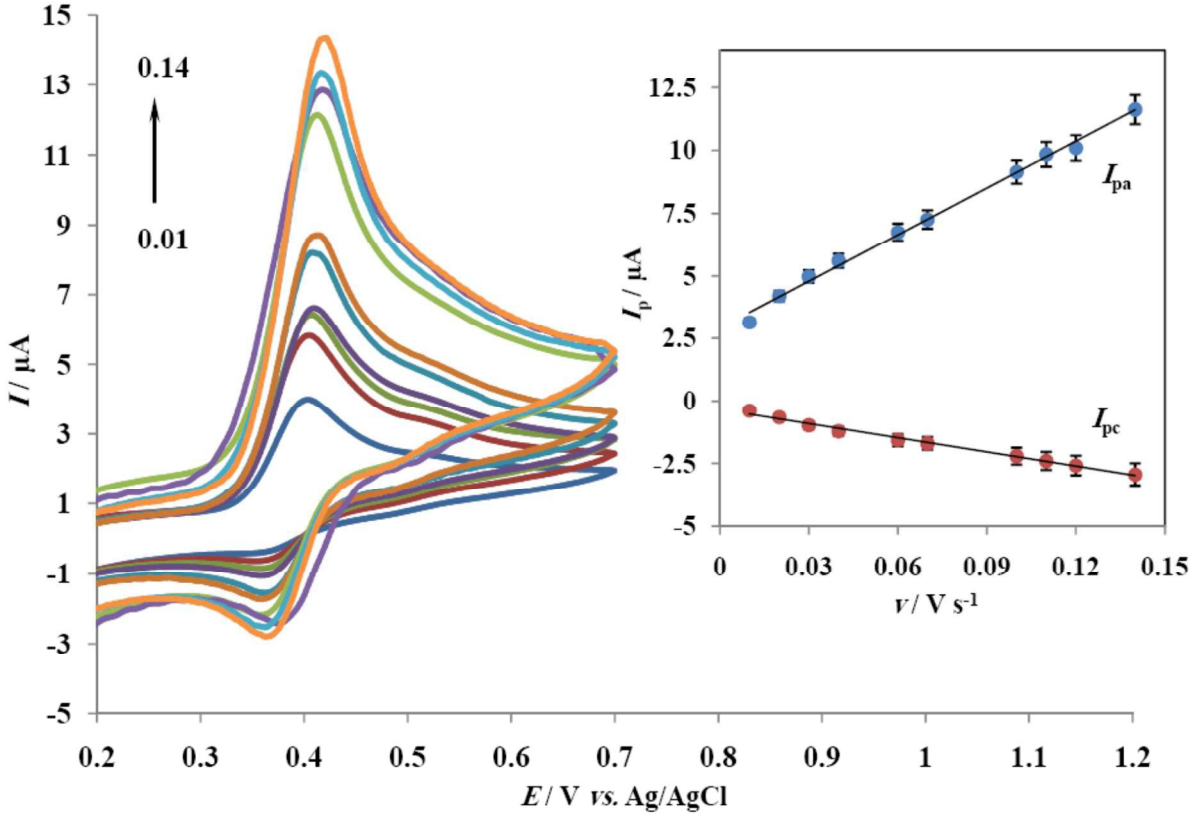

Figure 6

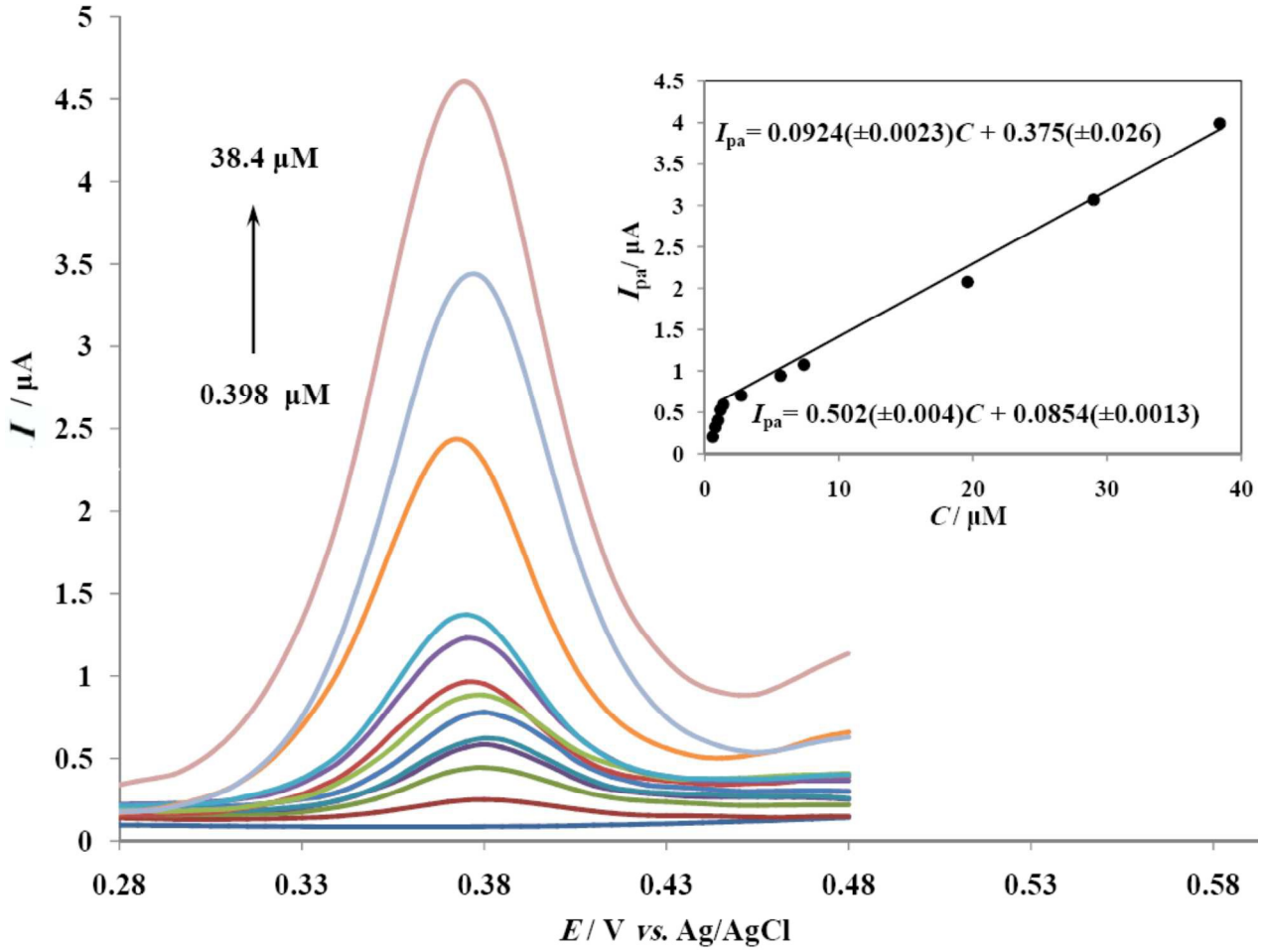

Figure 7

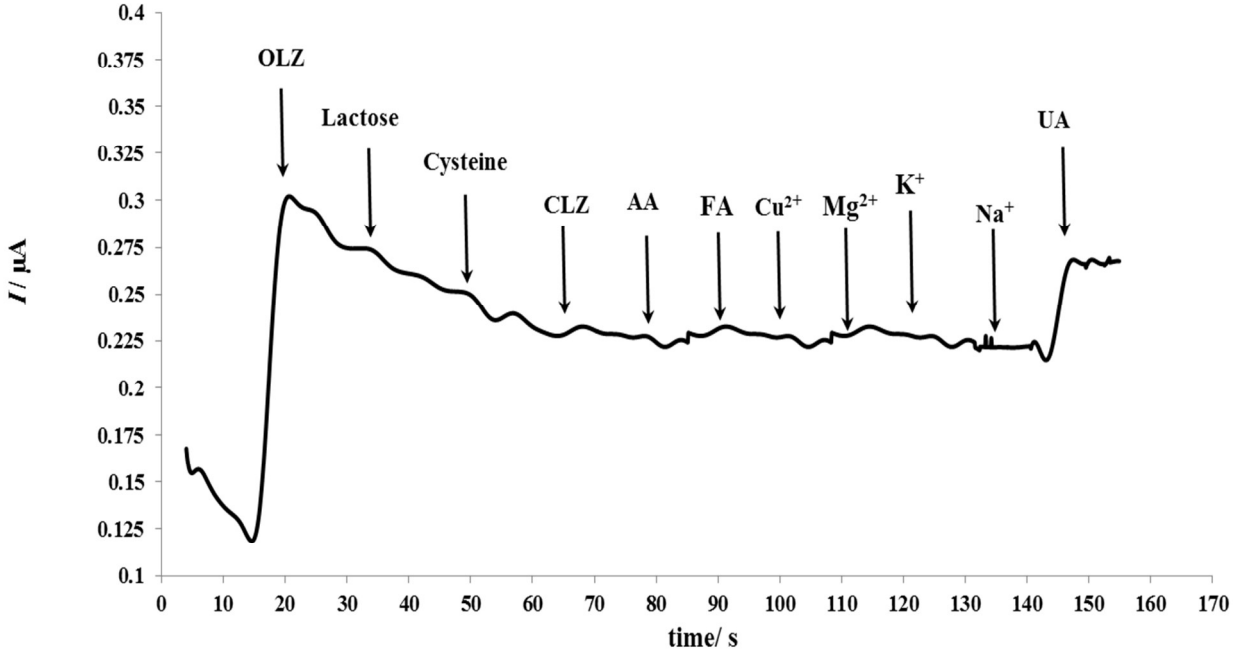

Figure 8